Proceedings of the 2008 International Manufacturing Science and Engineering Conference
MSEC2008
October 7-10, 2008, Evanston, Illinois, USA

MSEC_ICM&P2008-72532

DETERMINATION OF CUTTING FORCES FOR MICRO MILLING

Shih-Ming Wang, Department of Mechanical Engineering, Chung Yuan Christian University, shihming@cycu.edu.tw

Zou-Sung Chiang, Department of Mechanical Engineering, Chung Yuan Christian Universitys150@ms22.url.com.tw

Da-Fun Chen, Department of Mechanical Engineering, Chung Yuan Christian University, bigbigfunfun@yahoo.com.tw

Abstract

To enhance the implementation of micro milling, it is necessary to clearly understand the dynamic characteristics of micro milling so that proper machining parameters can be used to meet the requirements of application. By taking the effect of minimum chip thickness and rake angle into account, a new cutting force model of micro-milling which is function the instantaneous cutting area and machining coefficients was developed. According to the instantaneous rotation trajectory of cutting edge, the cutting area projected to xy-plane was determined by rectangular integral method, and used to solve the instantaneous cutting area. After the machining coefficients were solved, the cutting force of micro-milling for different radial depths of cut and different axial depths of cut can be predicted. The results of micro-milling experimental have shown that the force model can predict the cutting force accurately by which the optimal cutting parameters can be selected for micro-milling application.

Keywords: micro-milling, instantaneous projection area, depth of cut.

1 Introduction

Miniaturization with high-accuracy has been the design demand for many modern products. To fulfill the demand, micro manufacturing technology which can be applied to various applications needs to be developed. Because MEMS technology has its limit on manufacturing of complex 3D shape and variety of materials, many researchers have paid much attention for the development of non-MEMS micro manufacturing technology.

Micro milling can directly make miniature parts or produce molds for micro-forming process. Micro milling with the use of micro cutters (usually only 0.1-0.5 mm in diameter) usually performs at very high spindle speed (100,000 r.p.m. and up). With very small material removal rate, the dynamic behavior of micro milling is different from the regular milling process. In addition, because micro cutter is very thin, cutter deflection and vibration easily occur to cause deterioration of machining accuracy or even cutter broken. Thus, cutting forces should be proper controlled for micro milling process through the selection of optimal cutting parameters. The determination of optimal cutting parameters for micro milling needs to take the minimum chip thickness and, cutter geometry and machining efficiency into account so that the machining can be conducted with good accuracy and machining efficiency.

For regular milling, Tlusty and McNeil [1] had pointed out that the tangential cutting force is proportional to the cutting area that is function of chip thickness. Besides, the radial cutting force is also proportional to the tangential cutting force. Kuang-Hua Fuh et al [2] proposed a 2nd-order polynomial equation for the cutting force model. The model was function of four cutting parameters (spindle speed, feedrate, axial depth of cut, and radial depth of cut) which were determined based on lots of experimental data. The model could be accurate for machining when reliable experiments were conducted. Byung Guk et. al. [3] utilized finite element method to build the model for cutting dynamics. In the study, eccentric motion of tool was taken into account, and coordinate transformation was employed to identify the edge elements. When more information of tool material and tool structure was provided, the model can accurately explain the cutting dynamics. The results showed that it can predict cutting force with accuracy of 90%. Vogler et al [4] developed a cutting force model for composite materials. Basically the model was function of cutting area and material coefficients. According to the results of experiment using pure copper as a workpiece, Rahman et al [5] discovered that the chips generated by micro milling and regular milling would have same shape, but different sizes. In addition, the cutter life was dependent on helix angle of cutter, and the tangential cutting force is proportional to the axial cutting force. In 2005, Zaman et al [6] proposed a 3-D micro milling force model. The model determined the cutting force with calculation of the projected cutting area. However, because it can only approximately calculate the projected area, errors exist when cutting force was predicted. Besides, because the method needed to identify the cutting coefficients for each micro-milling with different axial depth of cut, it is not very convenient to apply for practical micro-milling application.

In this study, In this study, with taking the effect of minimum chip thickness and rake angle of cutter into consideration, a new approach for determination of micro milling forces was proposed. Furthermore, a method that can determine the micro-milling forces using same set of cutting coefficients for the applications with different axial depths of cut was addressed. The derived micro-milling force model was function of the instantaneous projected cutting area which can be solved when the projected instantaneous cutting area in xy-plane is known. Thus, the method to calculate the projected instantaneous cutting area was also developed in this study. Finally, verification experiments were conducted, and the experimental results were discussed.

2 Cutting force model

Figure 1 depicts the tangential cutting force, radial cutting, and axial cutting force. As shown in the figure, the direction of the tangential cutting force (F_t) is dependent upon the instantaneous rotation trajectory of cutter. The radial cutting force (F_r) pushes the cutting edge away from workpiece along x-direction. In the meanwhile, the axial cutting force (F_a) is acting along z-direction. The micro milling cutting forces for a fixed axial depth of cut model can be solved (Zaman et al [6]) as:

Tangential cutting force: $F_{ti} = K_m A_{pi}$ (1)

Radial cutting force: $F_{ri} = qF_{ti} + F_{elastic}$ (2)

Axial cutting force: $F_{zi} = -F_{ai} = -F_{ti}\sin\psi$ (3)

Where i represents the instantaneous cutting point on the cutting trajectory；A_{pi} represents instantaneous cutting area shown in Fig. 2；q represents proportional constant；ψ represents the helix angle of cutter; Km represents cutting coefficients. $F_{elastic}$ represents the force due to elastic deformation. Because the elastic strain occurred in the cutting experiment was very small, it was temporarily neglected here. Those coefficients can be determined based on a micro-milling experiment with a fixed axial depth of cut. Details of the procedure will be addressed later.

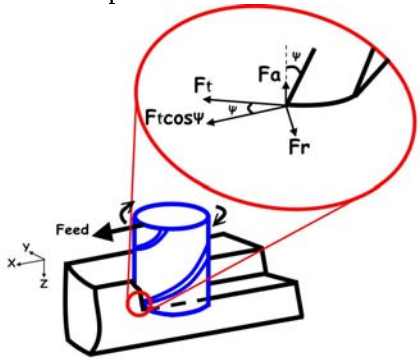

Fig.1 Illustrative of cutting forces

The instantaneous cutting area A_{pi} can be solved when the projected cutting area A_i that is the projection of A_{pi} on xy-plane (Fig. 2) is known. The relationship between A_i and A_{pi} is

$$A_{pi} = \frac{A_i}{\sin\psi} \quad (4)$$

When the projected cutting area A_i is known, it can be substituted into Eq. (4) to solve A_{pi}. F_{ti}, F_{ri}, and F_{ai} can, then, be solved according to Eq. (1)-(3).

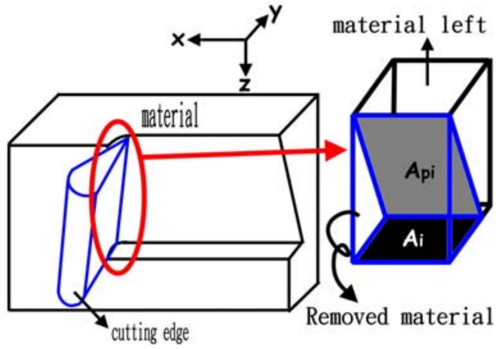

Fig. 2 Illustration of Projected cutting area

The cutting forces solved by Eq. (1), (2), and (3) can then be converted into the cutting forces in X, Y, and Z direction (as shown in Fig. 3). In Fig. 3, T1 and T2 were respectively the continuous rotation trajectory of cutter when the center of cutter was at o_1 and o_2, and φ_i represents the instantaneous rotation angle of the cutter. A and B are respectively the initial cutting points of trajectories T2 and T1. Point C is the intersection of T1 and T2. The cutting force in X丶Y丶Z direction can be expressed:

$$F_{xi} = (F_{ti}\cos\psi)\sin\varphi_i - F_{ri}\cos\varphi_i \quad (5)$$

$$F_{yi} = (F_{ti}\cos\psi)\cos\varphi_i - F_{ri}\sin\varphi_i \quad (6)$$

$$F_{zi} = -F_{ai} = -F_{ti}\sin\psi \quad (7)$$

3 Determination of projected cutting area

To use Eq. (1)-(3) to determine the cutting forces, the projected cutting area needs to be solved first. Area (ABC) (A_i) shown in Fig. 3 is the projected cutting area when the cutting edge moves along the planned T2. When material is cut, both elastic deformation and plastic deformation occur. The elastic deformation occurs within the region where the chip thickness is smaller than the minimum chip thickness, and the plastic deformation occurs in the region where the chip thickness is greater than the minimum chip thickness. The true projected cutting area in which material will be really cut should be equal to Area (ABC) (in Fig. 3) minus the elastic deformation area. The white area shown in Fig. 4 represents the true projected cutting area, and the red region is the elastic-deformation area. According to the model proposed by Seong Min Son [13], the minimum chip thickness t_m can be expressed as

$$t_m = r\left(1-\cos\left(\frac{\pi}{4}-\frac{\beta}{2}\right)\right) \qquad (11)$$

Where r is the radius of the cutter, and β represents the friction angle between cutter and workpiece which is also equal to the shear angle ϕ (Fig. 5). According to [7], the shear angle can be determined as following.

$$\phi = \tan^{-1}\left(\frac{\gamma\cos\alpha}{1-\gamma\sin\alpha}\right) = \beta \qquad (12)$$

$$\gamma = \frac{t}{t_c} \qquad (13)$$

Where t is depth of cut, and t_c is chip thickness.

Based on Eq. (11), (12) and (13), the minimum chip thickness can be solved and used to calculate the true projected cutting area., By taking the minimum chip thickness into account the true projected cutting area (shown Fig. 3 and 9) can be computed with using rectangular integral. The computation is independent with the instantaneous location of the cutting edge. According to the location of cutter tip, the true projected cutting area was differentiated into three cases:

(A) Case 1: Area (AA''B') (Fig.6) when $\varphi_A < \varphi_i \le \varphi_B$

In Fig. 4, A and A' are the cutting points on T2; B and B' are respectively the first cutting points on trajectories T1 and T2; L0 is the line connecting the first cutting point A and O_2; L1 is the line connecting the first cutting point B and O_2; L represents the line connecting the instant cutting point A'' on T2 and O_2; φ_i represents the instantaneous cutting angle between L and x-axis; and Y1 is the edge of workpiece that is parallel to x-axis.

Considering the effect of minimum chip thickness, the equation of T2 is as

$$(x - x_{o2})^2 + y^2 = r_e^{\,2} \qquad (13)$$

$$r_e = r - t_m \qquad (14)$$

For T2, the center of cutter locates at (vt, 0). v is the cutting federate, and t is the machining time. Therefore, $x_{o2} = vt = a_2$. If the tip of cutting edge locates in between A and A', the coordinates of any point on T2 are as $(r_e\cos\varphi_i + vt, r_e\sin\varphi_i)$. The equation of L is

$$\left(\tan[90^\circ - \varphi_i]\right)y - x = 0 \qquad (15)$$

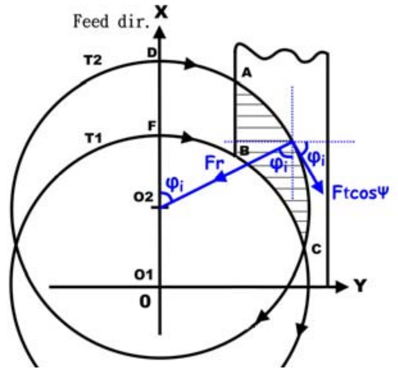

Fig. 3 Cutting Trajectories on X-Y plane

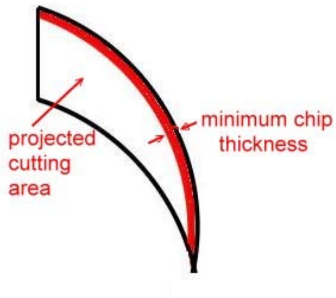

Fig. 4 Schematic of elastic-deformation region

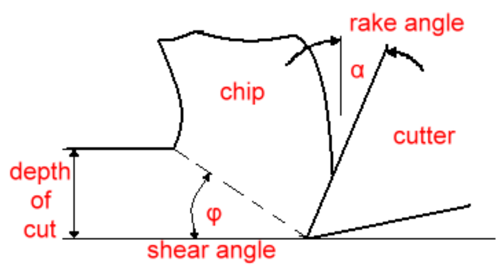

Fig. 5 Schematics of shear angle ϕ and rake angle

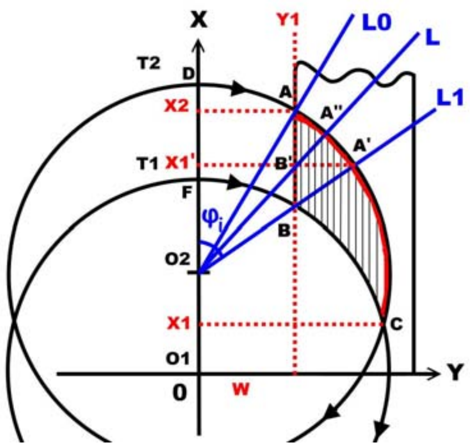

Fig. 6 Projected cutting area for $\varphi_A < \varphi_i \le \varphi_B$

Because the center of cutter is at (0, 0), the equation of T1 can be expressed as: $x^2 + y^2 = r_e^{\,2}$, where $y = w$. w represents the distance between the center of cutter and the edge of workpiece. Furthermore

$$x = \pm\sqrt{r_e^{\,2} - w^2} \tag{16}$$

According to Eq. (16), the coordinates of B is obtained as $\left(\sqrt{r_e^{\,2} - w^2}, w\right)$ and $\varphi_B = \tan^{-1}\left(\dfrac{w}{\sqrt{r_e^{\,2} - w^2} - vt}\right)$

$$\varphi_A = \sin^{-1}\left(\frac{w}{r_e}\right) \tag{17}$$

Finally, Area (AA''B') can be solved as

$$\begin{aligned}
A_{AA''B'} &= \int_w^{r\sin\varphi_i} (T2 - L)dy \\
&= \int_w^{r\sin\varphi_i} \left[\left(a_2 + \sqrt{r_e^{\,2} - y^2}\right) - (\cot\varphi_i)y\right]dy \\
&= vt(r_e \sin\varphi_i - w) + \frac{r_e^{\,2}}{2}\varphi_i - \frac{r_e^{\,2}}{2}\sin^{-1}\left(\frac{w}{r_e}\right) \\
&\quad - \frac{1}{2}w\sqrt{r_e^{\,2} - w^2} + \frac{1}{2}w^2\cot\varphi_i
\end{aligned} \tag{18}$$

(B) Case 2: Area (AA''C''B) (Fig. 7) when $\varphi_B < \varphi_i < 90^\circ$

When φ_i =90^o, L is normal to x-axis like L2, Area (AA''C''B) = Area(AA''D') – Area(BC''D'). Area(AA''D') can be solved as

$$\begin{aligned}
A_{AA''D'} &= \int_w^{r_e\sin\varphi_i} (T2 - L)dy \\
&= vt\,(r_e \sin\ \varphi_i - w) + \frac{r_e^{\,2}}{2}\varphi_i - \frac{r_e^{\,2}}{2}\sin^{-1}\left(\frac{w}{r_e}\right) \\
&\quad - \frac{1}{2}w\sqrt{r_e^{\,2} - w^2} + \frac{1}{2}w^2\cot\varphi_i
\end{aligned} \tag{19}$$

And, Area (BC''D') can be solved as

$$\begin{aligned}
A_{BC''D'} &= \int_w^{x_c\sin\varphi_i} (T1 - L)dy \\
&= \int_w^{x_c\sin\varphi_i}\left(\sqrt{r_e^{\,2} - y^2}\right)dy - \int_w^{x_c\sin\varphi_i}(\cot\varphi_i)ydy \\
&+ \frac{r_e^{\,2}}{2}\left[\frac{x_c\sin\varphi_i\sqrt{r_e^{\,2} - (x_c\sin\varphi_i)^2}}{r_e^{\,2}} - \frac{w\sqrt{r_e^{\,2} - w^2}}{r_e^{\,2}}\right] \\
&- \frac{1}{2}(\cot\varphi_i)\left[(x_c\sin\varphi_i)^2 - w^2\right]
\end{aligned} \tag{20}$$

According to Eq. (19) and (20), Area (AA''C''B) is obtained as

$$\begin{aligned}
A_{AA''D'} &= vt(r_e\sin\varphi_i - w) + \frac{r_e^{\,2}}{2}\varphi_i - \frac{r_e x_c}{2}\varphi_i \\
&- \frac{1}{2}x_c(\sin\varphi_i)\sqrt{r_e^{\,2} - (x_c\sin\varphi_i)^2} + \frac{1}{2}(\cot\varphi_i)(x_c^2\sin^2\varphi_i)
\end{aligned} \tag{21}$$

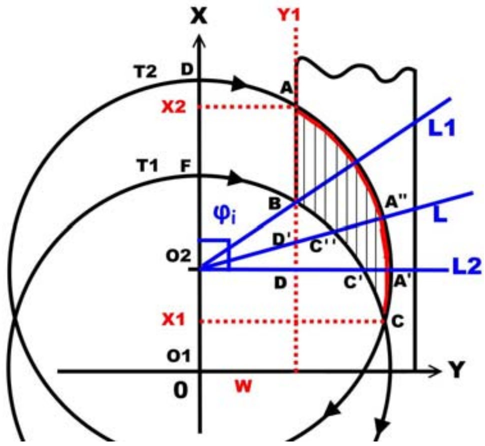

Fig. 7 Projected area when $\varphi_B < \varphi_i < 90^\circ$

(C) Case 3: Area (AA''C'B) (Fig. 8) when $90^\circ \le \varphi_i \le \varphi_c$,

Following similar procedures, it is noted that Area (AA''C'B) = Area (AGFB)+Area(FGA''C'). Area (AFGB) can be solved by Eq. (21). As shown in Fig. 8(b), Area (FGA''C') is the sum of Area(FHC'), Area(H I A''C'), and area(IGA''). Area (FHC') can be calculated as following.

$$\begin{aligned}
A_{FHC'} &= \int_{\sqrt{r_e^{\,2} - (vt)^2}}^{x_c\sin\varphi_i} (L2 - T1)dy \\
&= (vt)(x_c\sin\varphi_i) - \frac{vt}{2}\sqrt{r_e^{\,2} - (vt)^2} \\
&- \frac{r_e^{\,2}}{2}\left[\left(\frac{x_c\varphi_i}{r_e}\right) - \sin^{-1}\left(\frac{\sqrt{r_e^{\,2} - (vt)^2}}{r_e}\right)\right] \\
&- \frac{1}{2}x_c\sin\varphi_i\sqrt{r_e^{\,2} - (x_c\sin\varphi_i)^2}
\end{aligned} \tag{22}$$

Area (H I A''C') can be determined as

$$\begin{aligned}
A_{HIA'C'} &= \int_{x_c\sin\varphi_i}^{r\sin\varphi_i}(L2 - L)dy = \int\left[vt - (\cot\varphi_i)y\right]dy \\
&= (vt)(r_e - x_c)\sin\varphi_i - \frac{1}{2}(\cos\varphi_i)(r_e^{\,2} - x_c^2)(\sin\varphi_i)
\end{aligned} \tag{23}$$

Area(IGA'') can be determined as following:

$$\begin{aligned}
A_{IGA'} &= \int_{r_e\cos\varphi_i + vt}^{vt}(T2 - Y3)dx \\
&= \int_{r_e\cos\varphi_i + vt}^{vt}\left[\sqrt{r_e^{\,2} - (x - vt)^2} - r\sin\varphi_i\right]dx \\
&= \frac{r_e^{\,2}}{2}\left[(\sin\varphi_i)(\cos\varphi_i) + \tan^{-1}(-\cot\varphi_i)\right]
\end{aligned} \tag{24}$$

According to Eq. (20)-(22), Area (FGA''C') can be obtained as

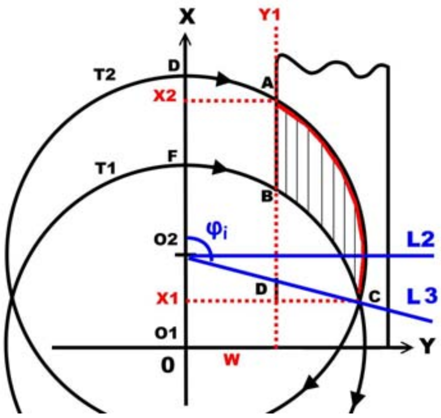

(a)

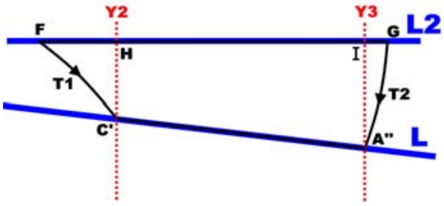

(b) enlarged figure of Area FGA"C'

Fig. 8 Projected cutting area when $90^\circ \le \varphi_i \le \varphi_c$

$$A_{\mathrm{FGA''C'}} = vt(r_e - w) + \frac{\pi r}{4}(r_e - x_c) - \frac{1}{2}x_c\sqrt{r_e^2 - x_c^2} - \left(\frac{vt}{2}\right)\sqrt{r_e^2 - (vt)^2} - \frac{r_e^2}{2}\left[\left(\frac{x_c}{r_e}\right)\varphi_i - \sin^{-1}\left(\frac{\sqrt{r_e^2 - (vt)^2}}{r_e}\right)\right] - \frac{1}{2}x_c\sin\varphi_i\sqrt{r_e^2 - (x_c\sin\varphi_i)^2} + (vt)r_e\sin\varphi_i \quad (25)$$

Finally, Area(AA"C'B) can be obtained as the sum of Area (AGFB) (Eq. (21)) and Area(FGA"C') (Eq. (25)).

4 Relationship between the axial depth of cut and the projected cutting area

The cutting force model is function of the instantaneous cutting area which is calculated based on the projected cutting area. When axial depth of cut is smaller than the spiral pitch of the flute, the projected cutting area is proportional to the axial depth of cut. When the axial depth of cut is greater than the spiral pitch of the flute, the projected cutting area will remains constant. However, the larger axial depth of cut is taken, the larger cutting force will be generated. Figure 9 shows the relationships between axial depth of cut, the helix angle ψ, and the spiral pitch (= L tanψ). Thus accumulating projected cutting area should be computed based on the axial depth of cut, and used for Eq. (4). When the axial depth of cut is set as H, Eq. (4) becomes

$$A_{pi} = \frac{A_i}{\sin\psi} \times \frac{H}{L \times \tan\psi} \qquad (26)$$

Where L is the circumference of the micro cutter; and ψ is the helix angle of the cuter.

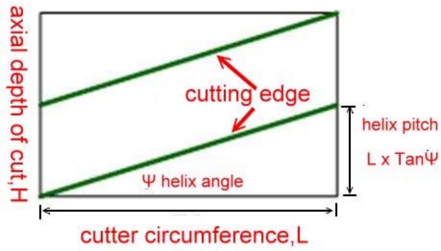

Fig. 9 Axial d.o.c. Vs. ψ & spiral pitch

5 Determination of K_m and q

Coefficients K_m and q should be determined by practical micro-milling experiments. First, the z-dir cutting force F_{zi} should be measured from the experiment. Subsequently, the tangential cutting force F_{ti} is solved based on Eq. (7). Then, K_m can be computed based on Eq. (1) with known cutting area A_{pi}. On the other hand, when F_{yi} is measured, the radial cutting force F_{ri} can, then, be solved from Eq. (6). By substituting F_{ri} into Eq. (2), coefficient q can be determined.

6 Experimental results

Equipments and instruments used for the experiment are listed in Table1. Micro end-mill with 0.5-mm diameter and copper were used. Table 2 lists the cutting parameters used for determination of K_m and q. In this experiment, the measured average maximum cutting forces in x-, y- and z-direction were respectively 1.1, 1.3, and 0.4 N (Fig. 10-12). The cutting area and projected cutting area were solved as A_i=9.605×10^{-6} mm^2 and A_{pi}=5.188×10^{-6} mm^2, respectively. According to the procedure aforementioned, K_m =77089.4 (N/mm^2) and q= 4.31567 were obtained.

To verify that the same set of k_m and q can be used for different axial depth of cuts, a micro-milling experiment with axial depth of cut=0.7 mm was conducted. The rest of cutting parameters for this experiment were the same as those in Table 2. The instantaneous cutting area and projected cutting area were 9.605×10^{-6} mm^2 and 6.0526×10^{-6} mm^2, respectively. Both of the simulated forces (computed by the model) and the measured cutting forces were listed in Table 3. Average maximum cutting forces were adopted for comparison. It was noted that the force model can predict the force with error less than 25%.

Another micro milling with different cutter diameter (ϕ=0.3 mm) and radial d.o.c. (= 0.1 mm) was also made. The rest of cutting parameters remained the same (Table 4). With same K_m and q, the simulated cutting forces were computed and compared with the measured cutting forces. It was found that the simulated cutting forces were very close to the actual (measured) cutting forces. The error of force simulation was less than 10%. The experimental results concluded that the proposed force model can accurately predict the micro milling forces with the same set of K_m and q.

Table 1 Equipment and instruments

Name	Type
Spindle	NSK HTS1501S-M2040 (150,000rpm)
Measurement Instrument	3-dir. force sensor: PCB 260A01 Frequency Analyzer: Portable PULSE - 3560C
machine	Toggle-type micro machine tool

Table2 Cutting parameters for determination of K_m & q

Axial d.o.c. = 0.6 mm	Material：copper
Radial d.o.c. = 0.2mm	Helix angle：45°
Spindle speed = 150,000rpm	Flutes：2
Feedrate = 15mm/min	Dia. of cutter = 0.5mm

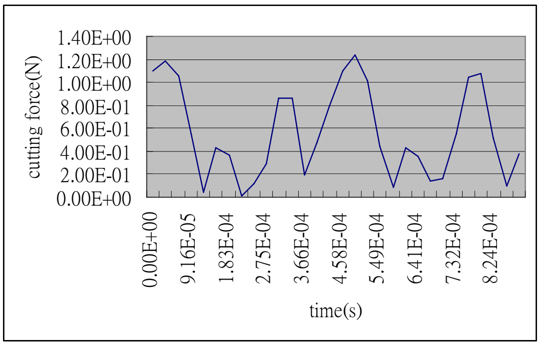

Fig. 10 Measures x-dir. Cutting force

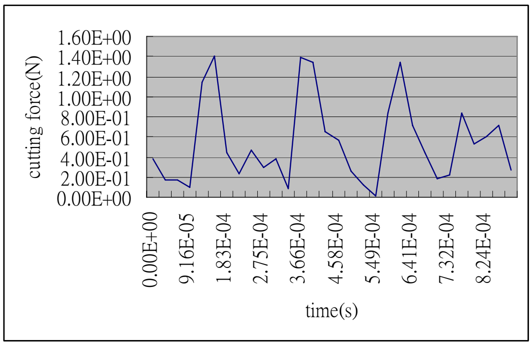

Fig. 11 Measured y-dir. Cutting force

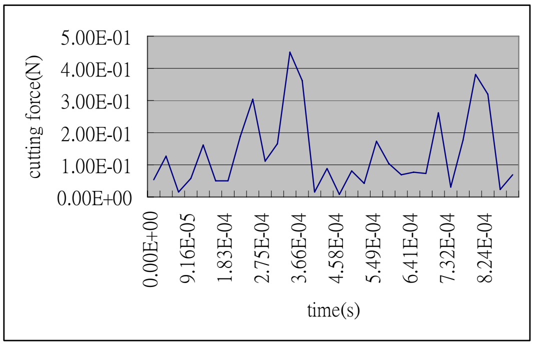

Fig.12 Measured z-dir. Cutting force

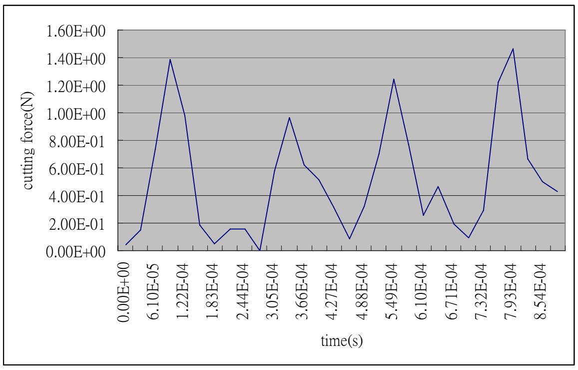

Fig. 13 X-dir. Cutting force

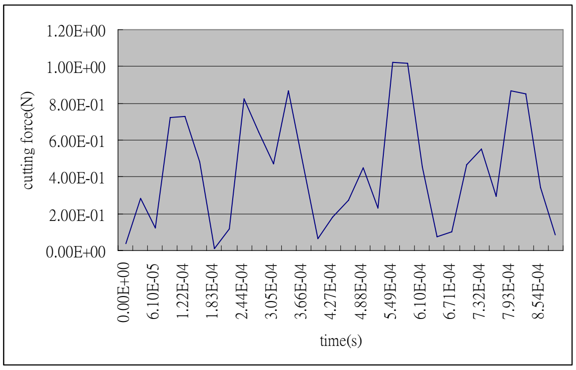

Fig. 14 Y-dir. Cutting force

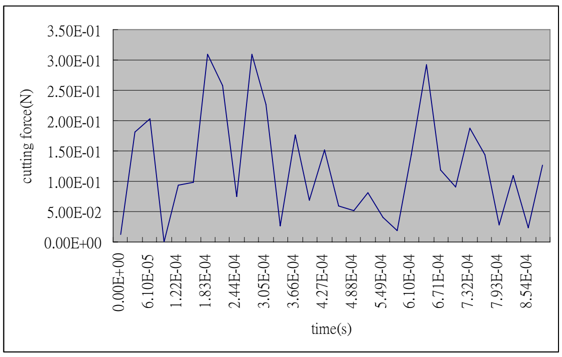

Fig. 15 Z-dir. Cutting force

Table 3 Forces for axial d.o.c.=0.7 mm

	Simulated max. force	Measured max. force
X-dir.	1.79794(N)	1.4(N)
Y-dir.	0.687291(N)	0.9(N)
Z-dir.	0.247487(N)	0.2(N)

Table 4 Cutting parameters for force model verification

Axial d.o.c. = 0.6mm	Material：copper
Radial d.o.c. = 0.1mm	Helix angle：45°
Spindle = 150,000rpm	flutes：2
Feedrate = 15mm/min	Dia. of cutter= 0.3mm

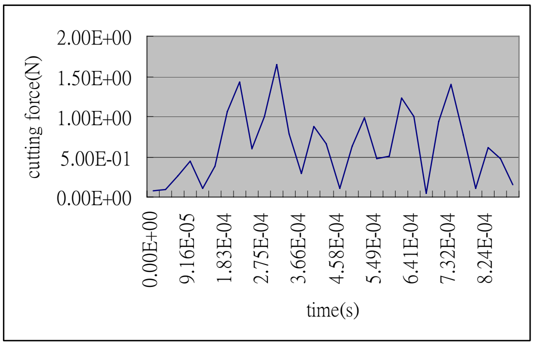

Fig. 16 X-dir. Cutting force

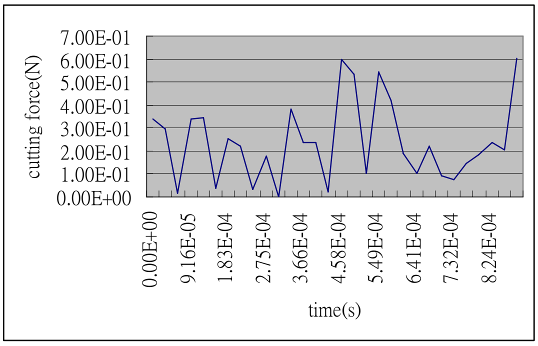

Fig. 17 Y-dir. Cutting force

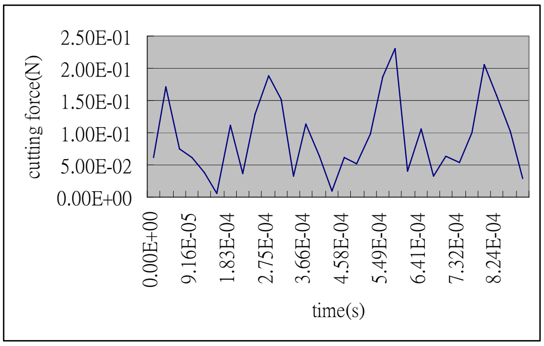

Fig. 18 Z-dir. Cutting force

Table 5 Forces for radial d.o.c=0.1 mm & ϕ=0.3 mm

	Simulated max. force	Measured max. force
X-dir.	1.31429(N)	1.2(N)
Y-dir.	0.455964(N)	0.5(N)
Z-dir.	0.180916(N)	0.25(N)

7 Conclusion

In this study, a new cutting force model that takes minimum chip thickness and rake angle into account was developed for micro milling. The derivation considers that the chip formation is composed of elastic deformation and plastic deformation. Minimum chip thickness was used to calculate the true cutting area where chip really deformed. With computing the instantaneous cutting area, the micro milling force can be determined. With same set of machining coefficients K_m and q, experimental results showed that the proposed model can predict the micro milling forces for different cutting condition with error less than 25%.

ACKNOWLEDGMENTS

This study is supported by National Science Council of the Republic of China under the grant number NSC 96-2745-E-033-006-URD.

Reference

[1] J. Tlusty, P. Maneil, “Dynamics of cutting force in end milling”, 1975, Annals of CIRP 24 (1) 21-25.

[2] Kuang-Hua Fuh and Ren-Ming Hwang, “A Predicted milling force model for high-speed end milling operation” 1997, Int. I. Mmch. Took Ma~fmct. Vol. 37, No. 7, pp. 969-979.

[3] Byung Guk Jun、Richard E. DeVor and Shiv G. Kapoor, , “Investigation of the dynamics of micro-end milling Part I: Model Development”. 1999, Department of Mechanical and Industrial Engineering

[4] Michael P. Vogler, Richard E. DeVor, Shiv G. Kapoor, , “Microstructure-level force prediction model for micro-milling of multi-phase materials” 2003,trans of the ASME Vol. 125 202-209.

[5] M. Rahman, A. Senthil Kumar, J.R.S. Prakash, , “Micro milling of pure copper”, 2001, Journal of Materials Processing Technology 116 39-43.

[6] M.T. Zaman, A. Senthil Kumar and M. Rahman, S. Sreeram , “A three-dimensional analytical cutting force model for micro end milling operation” 2005, International Journal of Machine Tools & Manufacture 46 353-336.

[7] Milton C. Shaw , “Metal Cutting Principles” 1996, Copyright 2004 Info Product Sites, Inc.